MOL-Eye: A New Metric for the Performance Evaluation of a Molecular Signal

Meriç Turan[1], Mehmet Şükrü Kuran[2], H. Birkan Yilmaz[3,4], Chan-Byoung Chae[4], Tuna Tugcu[1]
[1]Department of Computer Engineering, NETLAB, Bogazici University, Istanbul, Turkey
[2]Department of Computer Engineering, Abdullah Gul University, Kayseri, Turkey
[3]Department of Telematics Engineering, Universitat Politecnica de Catalunya, Barcelona, Spain
[4]School of Integrated Technology, Yonsei Institute of Convergence Technology, Yonsei University, Seoul, South Korea
E-mails:{meric.turan, tugcu}@boun.edu.tr, sukru.kuran@agu.edu.tr, birkan.yilmaz@upc.edu, cbchae@yonsei.ac.kr

***Abstract*—Inspired by the eye diagram in classical radio frequency (RF) based communications, the *MOL-Eye diagram* is proposed for the performance evaluation of a molecular signal within the context of molecular communication. Utilizing various features of this diagram, three new metrics for the performance evaluation of a molecular signal, namely the maximum eye height, standard deviation of received molecules, and counting SNR (CSNR) are introduced. The applicability of these performance metrics in this domain is verified by comparing the performance of binary concentration shift keying (BCSK) and BCSK with consecutive power adjustment (BCSK-CPA) modulation techniques in a vessel-like environment with laminar flow. The results show that, in addition to classical performance metrics such as bit-error rate and channel capacity, these performance metrics can also be used to show the advantage of an efficient modulation technique over a simpler one.**

***Index Terms*—Molecular communication, nanonetworks, communication via diffusion, vessel-like environments, eye diagram.**

I. Introduction

Nanonetworking is a communication paradigm that focuses on communication between nano-scale devices whose sizes are comparable to biological cells. Due to their small sizes, medical applications in in-vivo environments are expected to be one of the most prominent and driving application domains for these devices. However, an in-vivo environment is vastly different from classical radio frequency (RF) communication environments, and novel communication systems for this environment are needed to be developed. One such system is the molecular communication via diffusion (MCvD) that is based on relaying information over a diffusion channel using special molecules, called messenger molecules (MM) [1].

In the literature, the performance of an MCvD system is generally evaluated using either the signal-to-noise ratio (SNR), bit-error-rate (BER), or channel capacity. Less prominently, other metrics such as symbol-error-rate, signal-to-interference-noise-ratio (SINR), channel impulse response, and channel capacity considering transmitter energy budget have also been used. Previous studies which consider symbols that are representing multiple bits of information, utilize symbol-error-rate instead of BER [2], [3]. Other works that take into account the effect of interfering sources (e.g., inter-symbol interference (ISI), co-channel interference, adjacent channel interference) over the system use SINR instead of SNR [4], [5]. In [6]–[8], the authors use channel impulse response to show the effectiveness of the proposed signal shaping method. Lastly, channel capacity can also be expanded to include the energy limitation of the transmitter [9].

Among the three main metrics mentioned above, BER and channel capacity are defined in the context of MCvD. To the best of our knowledge the physical meaning of SNR and its calculation is not elaborated in detail in this new domain. In RF communication, as an alternative to SNR and SINR, a plot called eye diagram is also used to evaluate the performance of a signal. Different features of this diagram are used to measure various signal characteristics (i.e., eye opening for noise, eye width for jitter, and eye closure for ISI).

In this work, we propose a new diagram called MOL-Eye for evaluating the performance of a molecular signal. Specifically, we propose three performance metrics based on the MOL-Eye diagram as maximum eye height, standard deviation of the number of received molecules, and counting SNR to evaluate the performance of an MCvD system. We evaluate the validity of these performance metrics by comparing the performance of the classical binary concentration shift keying (BCSK) technique [3], [10] with an advanced modulation technique we call consecutive power adjustment (BCSK-CPA). BCSK-CPA is based on the power adjustment (BCSK-PA) technique proposed in previous works in the literature [11], [12]. According to our simulation results conducted in a 3D vessel-like environment, the three metrics proposed in the paper successfully depict the advantage of BCSK-CPA over BCSK, which shows the validity of the proposed metrics in the context of MCvD. Even though we consider a vessel-like environment, the eye diagram and the proposed performance metrics can also be applied to free diffusion environments.

The main contributions of the paper are summarized below:

- Based on the eye diagram concept in classical RF communications, we propose the MOL-Eye diagram in the context of MCvD.
- Using the MOL-Eye diagram, we introduce three new performance evaluation metrics the performance analysis of a molecular signal, i) maximum eye height– MaxEH, ii) standard deviation of the number of received molecules, and iii) counting SNR– CSNR.

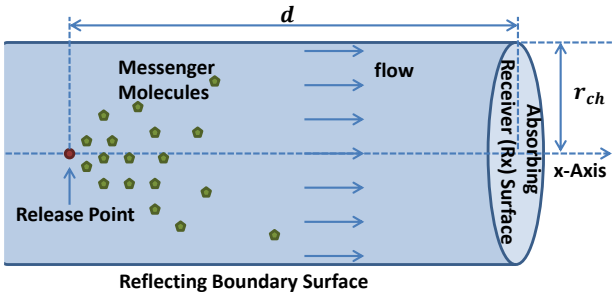

Fig. 1. Micro-fluidic based communication channel model representation

- We verify the applicability of these three metrics by comparing the performances of BCSK-CPA and basic BCSK techniques in MCvD.

II. System Model

Most prior work in the molecular communication literature considers a free diffusion environment where the MMs can roam freely without any boundaries (except the transmitter and the receiver) in the communication environment. In contrast, we consider a cylindrical (i.e., vessel-like) environment with a positive flow towards the receiver in this work. This vessel-like environment is more suitable to model significant *in-vivo* and *in-vitro* applications, e.g., sensing applications in blood vessels of a human body and micro-fluidic channels.

A. Diffusion Model

We consider a diffusion model consisting of a point transmitter, a fully absorbing circular receiver, a single type of information carrying MM, and a vessel-like environment with laminar flow. The vessel-like environment is considered to be a cylinder with a reflecting surface (Fig. 1). Since this is a closed environment with a positive flow towards the receiver, the surviving probability of MMs is much lower than the unbounded environment case (i.e., more MMs hit the receiver).

In the diffusion model, the total displacement along the x-axis (ΔX) of an MM in Δt duration is calculated as the sum of the displacement due to the flow (ΔX_{flow}) and displacement due to the diffusion ($\Delta X_{\text{diffusion}}$) as

$$\begin{aligned}\Delta X &= \Delta X_{\text{flow}} + \Delta X_{\text{diffusion}} \\ &= v_f\,\Delta t + \Delta X_{\text{diffusion}}\end{aligned} \tag{1}$$

where v_f is the laminar flow velocity.

Similar to the classical diffusion model without flow, the displacement due to diffusion follows a Gaussian distribution

$$\Delta X_{\text{diffusion}} \sim \mathcal{N}(0, 2D\Delta t) \tag{2}$$

where Δt is the simulation time step, D is the diffusion coefficient, and $\mathcal{N}(\mu, \sigma^2)$ is the Gaussian random variable with mean μ and variance σ^2. Considering the movement in all three axes, the total displacement in a single time step is calculated as:

$$\overrightarrow{r} = (\Delta X, \Delta Y, \Delta Z) \tag{3}$$

where ΔY and ΔZ correspond to the displacement in the y- and the z-axes, respectively, both of which follow a Gaussian distribution with the same μ and σ values with $\Delta X_{\text{diffusion}}$.

B. Modulation and Demodulation

In this study, we use binary concentration shift keying (BCSK) as the modulation technique with a symbol duration of t_s [10]. In BCSK, a given symbol at the k^{th} symbol duration (i.e., $S[k]$) can either represent bit-0 or bit-1 (i.e., $S[k] \in \{0, 1\}$). Based on this value, the transmitter releases $N^{\text{Tx}}[k]$ MMs where $N^{\text{Tx}}[k] = n_{S[k]}$. In order to increase the detectability of bit-0s and bit-1s, we choose n_0 as 0 and n_1 as the sufficient number of molecules.

At the receiver side, $N^{\text{Rx}}[k]$ represents the number of MMs arriving at the receiver within the k^{th} symbol slot, which includes both MMs from the current symbol and the previous symbols. As in (4), the receiver applies a basic thresholding on $N^{\text{Rx}}[k]$ to decode the signal ($\hat{S}[k]$) as either bit-0 or bit-1.

$$\hat{S}[k] = \begin{cases} 0, & N^{\text{Rx}}[k] < \lambda \\ 1, & N^{\text{Rx}}[k] \geq \lambda \end{cases} \tag{4}$$

In addition to the basic BCSK technique we have also implemented a variant of BCSK with power adjustment (BCSK-PA) technique proposed in [12] that we call BCSK with consecutive power adjustment (BCSK-CPA). BCSK-PA focuses on minimizing the variation between the $N^{\text{Rx}}[k]$ values where $S[k]=1$, regardless of the values of the past m symbols (where m is the number of past symbols that are assumed to be affecting the current symbol, which is also called as the ISI window length) by regulating the molecular emission rate. By doing so, BCSK-PA aims to considerably reduce the effect of ISI in MCvD. To this end, in BCSK-PA the transmitter uses emission rates based on past symbol values as $\boldsymbol{H}_k^m$ where $\boldsymbol{H}_k^m = (S[k-1], S[k-2], ..., S[k-m])$ is a vector representing the symbol values of the previous m symbols at the k^{th} symbol slot (i.e., the history of bits at the k^{th} symbol slot).

Although BCSK-PA reduces the ISI effect in the communication, it requires a considerable amount of memory at the transmitter side, especially as m increases (e.g., BCSK-PA with $m = 10$ requires 1024 distinct $\boldsymbol{H}_k^m$ cases and corresponding emission amounts). Our new technique, BCSK-CPA, aims reducing this memory requirement by only considering the cases where the previous symbols have consecutive bit-1s to change the emitted MM count. Fig. 2 shows the state diagram of a transmitter utilizing BCSK-CPA with m-memory where the state number represents the consecutive bit-1s. Also, $\boldsymbol{C}_k$ replaces $\boldsymbol{H}_k^m$ from CSK-PA and denotes the number of consecutive bit-1s just before the k^{th} symbol slot as

$$\boldsymbol{C}_k = \begin{cases} 0, & S[k-1]=0 \\ 1, & S[k-2]=0\,,\ S[k-1]=1 \\ 2, & S[k-3]=0\,,\ S[k-2]=1\,,\ S[k-1]=1 \\ . & . \\ m, & \forall i\ k-m \leq i < k\ S[i]=1 \end{cases} \tag{5}$$

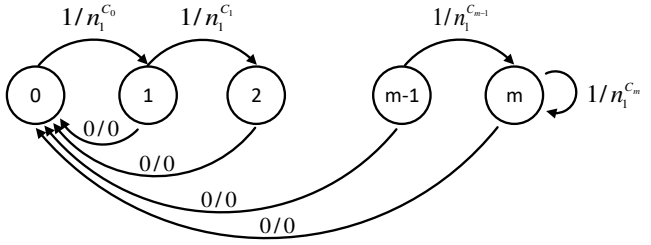

Fig. 2. State diagram of BCSK-CPA. The state diagram counts the consecutive bit-1s until the current bit. State transitions are given in the form of r/o, where r and o represent $S[k]$ and the $N^{\text{Tx}}[k]$, respectively (e.g., if $S[k]=1$ when the state is 1, the new state becomes 2 and $n_1^{C_1}$ molecules will be emitted in the current symbol slot).

The rationale behind BCSK-CPA depends on the fact that in a BCSK system, the effect of bit-0s over ISI is zero. Therefore, we can omit the effect of bit-0s in the past symbol values to reduce the memory requirements of the technique while not considerably impairing the performance of the system.

When molecules are emitted from the emission point, some of them hit the receiver in the current symbol slot while the rest resides in the channel and can be received during the successive symbol slots. We define p_i as the mean fraction of emitted molecules that are received during the i^{th} following symbol slot. Please note that p_0 corresponds to the mean fraction of molecules to be absorbed during the current symbol slot. Therefore, the expected number of molecules to be absorbed in the k^{th} symbol slot becomes

$$\mathbf{E}(N^{\text{Rx}}[k]) = p_0 N^{\text{Tx}}[k] + \underbrace{\sum_{i=1}^{m} p_i N^{\text{Tx}}[k-i]}_{\text{residual}} \tag{6}$$

where $\mathbf{E}(\cdot)$ is the expectation operator.

For BCSK-CPA, the number of molecules to emit is adjusted according to the number of consecutive bit-1s as explained above. Therefore, the expected number of residual molecules ($N_{\text{residual}}[k]$) for the k^{th} symbol slot becomes

$$\mathbf{E}(N_{\text{residual}}[k]) = \sum_{i=1}^{\boldsymbol{C}_k} p_i N^{\text{Tx}}[k-i]. \tag{7}$$

Please note that $\mathbf{E}(N_{\text{residual}}[k])$ can be calculated by the transmitter since the transmitted bits are known perfectly. Hence, the number of molecules to emit is adjusted as

$$N^{\text{Tx}}[k] = \begin{cases} n_0 & S[k]=0 \\ n_1^{\boldsymbol{C}_k} = n_1^{\boldsymbol{C}_0} - \frac{\mathbf{E}(N_{\text{residual}}[k])}{p_0} & S[k]=1 \end{cases} \tag{8}$$

where $n_1^{\boldsymbol{C}_k}$ denotes the number of molecules to emit when the number of consecutive bit-1s is $\boldsymbol{C}_k$. Note that this scheme ensures to have approximately the same expected number of molecules (at the receiver side) for each bit-1, namely $p_0\, n_1^{\boldsymbol{C}_0}$, which is equal to $p_0\, n_1$.

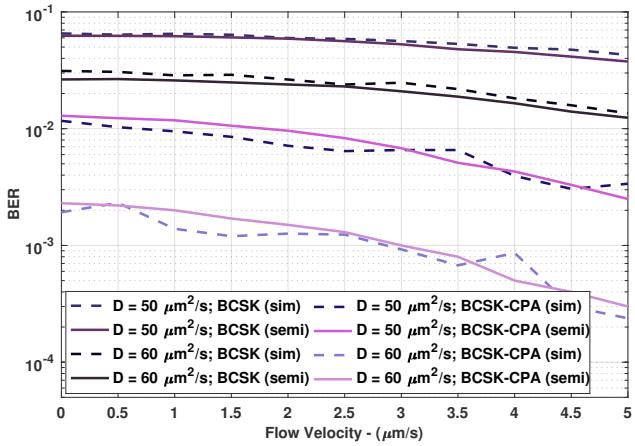

Fig. 3. BER plot for BCSK and BCSK-CPA. Curves with the name *sim* and *semi* correspond to the simulation and the semi analytical method. ($d = 6\,\mu\text{m}$, $n_1 = 300$, $t_s = 0.4\,\text{s}$)

C. BER Formulation with and without CPA

In (6), the expected number of received molecules at symbol slot k is given, and $N^{\text{Rx}}[k]$ exhibits a binomial random variable [13]. For tractability, we approximate the binomial random variables with a Gaussian random variable as

$$\begin{aligned} N^{\text{Rx}}[k] &\sim \mathcal{N}(\mu_k, \sigma_k^2) \\ \mu_k &= \sum_{i=0}^{m} p_i\, N^{\text{Tx}}[k-i] \\ \sigma_k^2 &= \sum_{i=0}^{m} p_i\,(1-p_i)\, N^{\text{Tx}}[k-i] \end{aligned} \tag{9}$$

where $N^{\text{Tx}}[k-i]$ differs for BCSK-CPA and BCSK. We acquire the p_i values by simulation. Then, we can evaluate the probability of error ($\mathbf{P}_e$) by using Gaussian distribution tail probabilities. Considering the history that includes the previous bits, we obtain $\mathbf{P}_e$ at the k^{th} symbol slot as

$$\begin{aligned} \mathbf{P}_e = \mathbf{P}_{e|S[k]=0,\boldsymbol{H}_k^{k-1}}\, \mathbf{P}(S[k]=0, \boldsymbol{H}_k^{k-1}) \\ + \mathbf{P}_{e|S[k]=1,\boldsymbol{H}_k^{k-1}}\, \mathbf{P}(S[k]=1, \boldsymbol{H}_k^{k-1}) \end{aligned} \tag{10}$$

where $\mathbf{P}_{e|S[k],\boldsymbol{H}_k^{k-1}}$ corresponds to the probability of error given that the history bits are $\boldsymbol{H}_k^{k-1}$ and the current bit is $S[k]$. We evaluate these probabilities with the tail probabilities of the approximate arrival distribution (i.e., the random variable in (9)) and considering only the ISI window (i.e., $\boldsymbol{H}_k^m$). Please note that we do not need all of the previous bit values to implement BCSK-CPA. However, we need these bit values for the evaluation of BER for analysis purposes.

In Fig. 3, we plot the flow velocity versus BER values for the two modulation techniques (i.e., BCSK and BCSK-CPA) considering two different D values. In all cases, the simulation and analytical method values are coherent with each other (i.e., simulation results are validated by the analytical method values). Moreover, as expected BCSK-CPA outperforms BCSK by a considerable margin. Additionally, the results show that BER and laminar flow is inversely proportional to one another.

III. Eye Diagram and MOL-Eye Diagram

Eye diagram is a method for measuring the quality of a signal [14]. The name of eye diagram comes from its shape. The width of the eye defines the time interval of the received signal without ISI. Therefore, the more the eye is open, the less the ISI level is, and vice versa. Eye diagrams, obtained by using oscilloscope, are mostly used by field engineers. Eye diagram is useful for detecting problems such as noise, jitter, and attenuation. The conventional eye diagram has five metrics that are also applicable in MC:

- *0 and 1 level*: The mean values of bit-0 and bit-1 curves in the diagram (dashed lines in Fig. 7).
- *Rise and fall time*: Transition times of the data to the upward and downward slope of the eye diagram.
- *Eye amplitude*: The biggest distance between the mean of bit-0 and the mean bit-1 curves.

In the context of molecular communication (MC), we propose MOL-Eye as analogous to the eye diagram in conventional communications. MOL-Eye is a good way to visualize signals in MC, as can be seen in Fig. 7. To obtain the eye diagrams in the figure, the received signals of consecutive bit transmissions are repetitively sampled and applied in an overlapping fashion. Moreover, curves of bit-1 transmissions are in dark blue whereas bit-0s' are in light blue. The diagrams in the first row are generated using the BCSK technique, whereas the diagrams in the second row are generated using the BCSK-CPA technique. Also, environmental conditions get worse from left to right, and consequently the openness of the MOL-Eye starts to decrease.

In the MC literature, BER is used extensively to measure the quality of the signal. However, BER calculation requires excessive processing power, which would be unsuitable for nanomachines that are expected to have very low energy budgets. Therefore, we propose three performance metrics derived from MOL-Eye diagram as alternative performance metrics. We use the conventional eye diagram metric called, maximum eye height (MaxEH), as well as propose two new metrics for the molecular signal, namely the standard deviation of the received molecules and counting SNR (CSNR). Especially, CSNR is a promising metric since we observe a one-to-one relation between CSNR and BER. Therefore, if the relation between BER and CSNR can be formulated, BER evaluation and optimization process will be much more efficient.

In this work, we propose CSNR as a supportive metric to BER. To calculate CSNR, we first define the integral difference between every combination of bit-1 and bit-0 curves as in (11)

$$\Delta_c(i,j) = \int_0^{t_s} c_1(i) - c_0(j)\, dt \tag{11}$$

where $c_1(i)$ and $c_0(j)$ are the i^{th} bit-1 and j^{th} bit-0 sampled curves, and t_s is the symbol duration. Consequently, we calculate the mean, μ_{Δ_c}, and the standard deviation, $STD(\Delta_c)$, of Δ_c values. Finally, we calculate CSNR as in

$$CSNR = \frac{\mu_{\Delta_c}}{STD(\Delta_c)}, \tag{12}$$

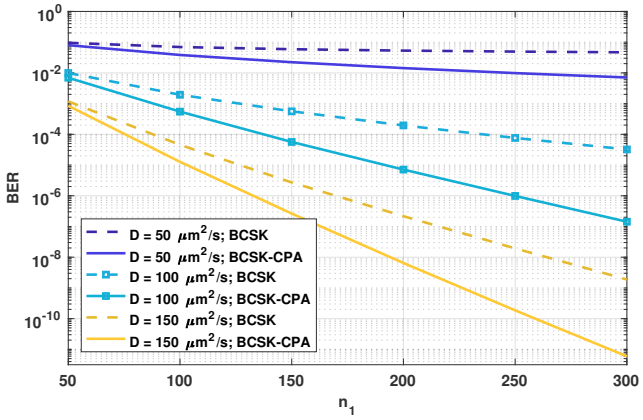

Fig. 4. Number of molecules vs. BER ($d = 6\,\mu$m, $v_f = 0$, $t_s = 0.4\,$s)

which is an alternative definition of SNR for non-negative signals [15]. As explained above, MC utilizes MMs and considers the received number of MMs as the signal (i.e., molecular signals are non-negative signals). Therefore, this alternative SNR definition fits quite well to MC.

IV. Numeric Results

The results presented in this section are obtained from the custom-made simulator that keeps track of the hitting molecules, which is the number of successfully received molecules in every simulation time step. By utilizing the simulation output, we evaluate the aforementioned eye diagram metrics and BER values under different conditions.

We consider MCvD in a vessel-like environment as depicted in Fig. 1. The system parameters are given in Table I.

TABLE I
Simulation Parameters

Parameter	Value
Radius of channel (r_{ch})	$5\,\mu$m
Radius of the receiver	$5\,\mu$m
Distance between Tx and Rx (d)	$\{4, 5, 6\}\mu$m
Diffusion coefficients (D)	$\{50, 100, 150\}\mu\text{m}^2/\text{s}$
Laminar flow velocities (v_f)	$0 \sim 5\mu\text{m/s}$
Simulation time step (Δt)	$0.1\,$ms
n_1 (BCSK), $n_1^{C_0}$ (BCSK-CPA)[a]	$50 \sim 300$
Symbol duration (t_s)	$\{0.4, 0.5\}$s
Length of bit sequence	100 bits
Number of replications	250

[a] In the rest of this section, for the sake of simplicity, we refer to both of these parameters simply as n_1.

A. BER Analysis

In Fig. 4, BER values corresponding to various D values, n_1 values, and modulation techniques are presented. According to the figure, BER decreases as D and n_1 increase. Note that the relative gain of BCSK-CPA compared to BCSK is greater for higher D values.

Since CSNR represents the quality of the signal across noise, it is also expected to be inversely proportional to BER.

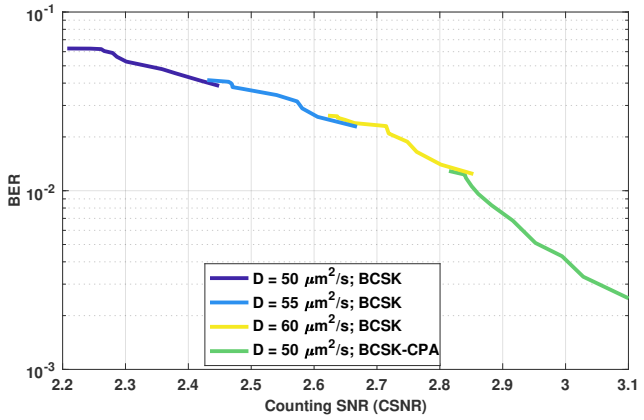

Fig. 5. CSNR vs. BER ($d = 6\,\mu\text{m}$, $v_f = 0$, $n_1 = 300$, $t_s = 0.4\,\text{s}$)

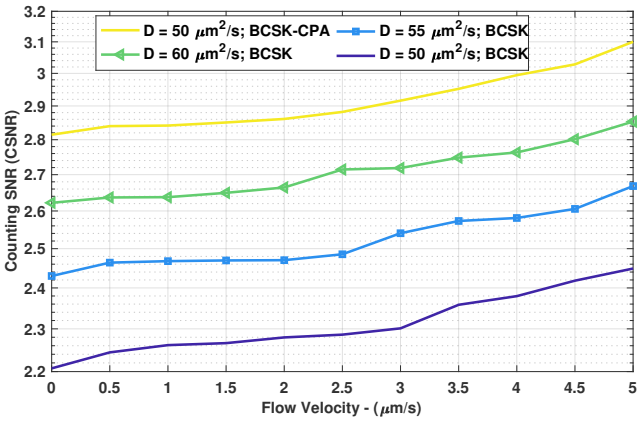

Fig. 6. Flow velocity vs. CSNR ($d = 6\,\mu\text{m}$, $n_1 = 300$, $t_s = 0.4\,\text{s}$)

We validate this by running simulations for 11 different flow values from $0\,\mu\text{m/s}$ to $5\,\mu\text{m/s}$ that are sequentially increased by $0.5\,\mu\text{m/s}$, three different D values, and two different modulation techniques: BCSK and BCSK-CPA (Fig. 5). Finally, the relation between CSNR and BER is injective for the given parameters, which means BER can be formulated in terms of CSNR - if the derivations are tractable and can be formulated, BER calculations for CSK-based modulations will be eased. For the future work, we will focus on the analytical derivation of the relation between CSNR and BER.

B. Eye Diagram Analysis

In the context of MC, we define three new metrics, which are standard deviation of the number of received molecules, STD($c_0(:)$) and STD($c_1(:)$), MaxEH, and CSNR. The standard deviation is simply calculated by quantifying the amount of variation in the number of received molecules. MaxEH is the maximum distance between the curves of a bit-0 and bit-1 in a single symbol slot. In (11) and (12), the steps of CSNR calculation are depicted.

In order to test the proposed metrics under different circumstances, we define three different environmental conditions by differing the D inspired by [9]. Moreover, d and v_f values are inspired by the thinnest part of the capillaries [16]. The defined parameters which are named as good, moderate, and harsh can be seen in Table II.

TABLE II
ENVIRONMENT PARAMETERS FOR THE EYE DIAGRAM ANALYSIS

Environments	$d(\mu\text{m})$	$D(\mu\text{m}^2/\text{s})$	$v_f(\mu\text{m/s})$
Good	4	150	5
Moderate	5	100	2.5
Harsh	6	50	0

Table III shows the STD($c_0(:)$), STD($c_1(:)$), MaxEH, and CSNR values in these three environments. As seen in the table, MaxEH and CSNR increase while the environment gets better or when BCSK-CPA method is used. For the calculation of MaxEH, we normalize the total number of received molecules. For ease of comparison, the metric values of BCSK-CPA in the good environment are given in a bold face font, which represent the best results among six different conditions.

TABLE III
METRICS OF EYE DIAGRAM

Environments	Metric Name	with CPA	w/o CPA
Good	STD($c_0(:)$)	**11.0948**	11.5592
	STD($c_1(:)$)	**29.3192**	29.8338
	MaxEH	**127.6994**	118.0000
	CSNR	**14.5762**	11.6322
Moderate	STD($c_0(:)$)	13.8048	15.1311
	STD($c_1(:)$)	27.2424	29.1996
	MaxEH	68.0454	65.0000
	CSNR	8.5072	6.6060
Harsh	STD($c_0(:)$)	16.0739	19.7512
	STD($c_1(:)$)	22.7202	27.6683
	MaxEH	38.3462	36.0000
	CSNR	3.6683	2.8110

Fig. 6 depicts the effect of flow velocities over D values and modulation techniques. As seen in this figure, unlike the relation between BER and flow velocity as in Fig. 3, CSNR rises with increasing flow velocity as expected.

Finally, the eye diagrams for three different environmental conditions can be seen in Fig. 7. The widths are wider in the good environment compared to the moderate and the harsh environments, which shows that the effect of ISI is less in good environment. Moreover, the eyes are also more open in the good environment than the moderate and harsh the environments, which shows that there is less noise in the good environment. Please note that the received signals in Fig. 7 are obtained from consecutive transmissions and they include ISI.

V. CONCLUSION AND FUTURE WORK

In this paper, we have proposed a new metric called MOL-Eye based on the conventional eye diagram concept. We introduced three new metrics for performance evaluation using derivatives of MOL-Eye i.e., i) MaxEH, standard deviation of the number of received molecules, and CSNR. We showed that these metrics can be used to exhibit the quality of different performance enhancement methods in MC (i.e., BCSK vs.

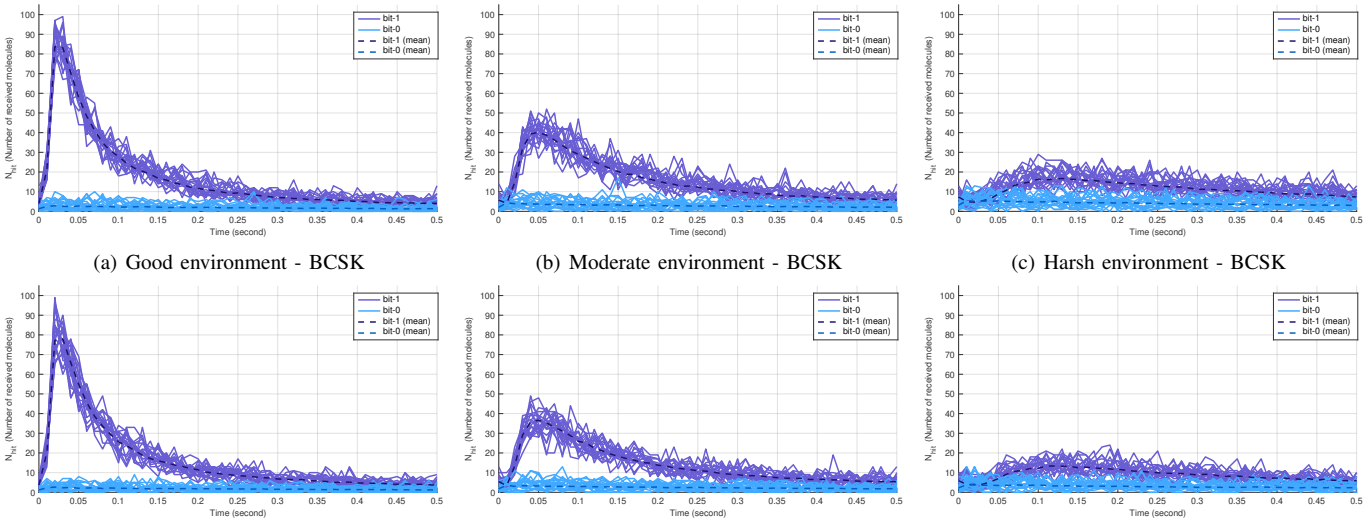

(a) Good environment - BCSK (b) Moderate environment - BCSK (c) Harsh environment - BCSK

(d) Good environment - BCSK-CPA (e) Moderate environment - BCSK-CPA (f) Harsh environment - BCSK-CPA

Fig. 7. MOL-Eye diagrams of consecutive bit transmissions in different environmental conditions for both with and without CPA cases ($t_s = 0.5\,\mathrm{s}$).

BCSK-CPA). In our experiments, we considered a vessel like environment with laminar flow under three different environmental conditions (i.e., good, moderate, harsh) for two different modulation techniques, namely conventional BCSK and BCSK-CPA (which was also proposed in this paper as an alternative power adjustment method to BCSK-PA). When we compared the performances under different conditions, we confirmed that BCSK-CPA outperforms BCSK and the good environment case outperforms the moderate and harsh cases, and so on as expected. Based on our evaluations, we have also seen that CSNR is inversely proportional with BER as in Fig. 5. Moreover, CSNR and BER have one-to-one relation, which points out that BER can be formulated in terms of CSNR. As a future work, we plan to analyze the complexity of the metrics and find the analytical derivation of the relation between CSNR and BER.

Acknowledgment

This research was partially supported by the Scientific and Technical Research Council of Turkey (TUBITAK) under Grant number 116E916, the Basic Science Research Program (2016K2A9A1A06926542, 2017R1A1A1A05001439) through NRF of Korea, and by Generalitat de Catalunya of the Secretariat for Universities and Research of the Ministry of Business and Knowledge of the Government of Catalonia via the Beatriu de Pinos program.

References

[1] N. Farsad, H. B. Yilmaz, A. Eckford, C.-B. Chae, and W. Guo, "A comprehensive survey of recent advancements in molecular communication," *IEEE Commun. Surveys Tuts.*, vol. 18, no. 3, pp. 1887–1919, 2016.

[2] A. Singhal, R. K. Mallik, and B. Lall, "Performance analysis of amplitude modulation schemes for diffusion-based molecular communication," *IEEE Trans. Wireless Commun.*, vol. 14, no. 10, pp. 5681–5691, Oct. 2015.

[3] N.-R. Kim and C.-B. Chae, "Novel modulation techniques using isomers as messenger molecules for nano communication networks via diffusion," *IEEE J. Sel. Areas in Commun.*, vol. 31, no. 12, pp. 847–856, Dec, 2013.

[4] P. Raut and N. Sarwade, *Connectivity Model for Molecular Communication-Based Nanomachines Network in Normal and Sub-diffusive Regimes*. New Delhi: Springer India, 2016, pp. 245–256.

[5] V. Jamali, A. Ahmadzadeh, and R. Schober, "On the design of matched filters for molecule counting receivers," *IEEE Commun. Lett.*, vol. 21, no. 8, pp. 1711–1714, Aug. 2017.

[6] M. U. Mahfuz, D. Makrakis, and H. T. Mouftah, "On the characterization of binary concentration-encoded molecular communication in nanonetworks," *Elsevier Nano Commun. Netw.*, vol. 1, no. 4, pp. 289 – 300, 2010.

[7] S. Wang, W. Guo, and M. D. McDonnell, "Transmit pulse shaping for molecular communications," in *Proc. IEEE Int. Conf. on Comput. Commun. Workshops (INFOCOM WKSHPS)*, April 2014, pp. 209–210.

[8] C. T. Chou, "Molecular circuits for decoding frequency coded signals in nano-communication networks," *Elsevier Nano Commun. Netw.*, vol. 3, no. 1, pp. 46 – 56, 2012.

[9] M. S. Kuran, H. B. Yilmaz, T. Tugcu, and B. Ozerman, "Energy model for communication via diffusion in nanonetworks," *Elsevier Nano Commun. Netw.*, vol. 1, no. 2, pp. 86 – 95, 2010.

[10] M. S. Kuran, H. B. Yilmaz, T. Tugcu, and I. F. Akyildiz, "Modulation techniques for communication via diffusion in nanonetworks," in *Proc. IEEE Int. Conf. on Commun. (ICC)*, Jun. 2011, pp. 1–5.

[11] A. Einolghozati, M. Sardari, A. Beirami, and F. Fekri, "Capacity of discrete molecular diffusion channels," in *Proc. IEEE Int. Symp. on Inf. Theory (ISIT)*, Jul. 2011, pp. 723–727.

[12] B. Tepekule, A. E. Pusane, H. B. Yilmaz, and T. Tugcu, "Energy efficient ISI mitigation for communication via diffusion," in *Proc. IEEE Int. Black Sea Conf. on Commun. and Netw. (BlackSeaCom)*, May 2014, pp. 33–37.

[13] H. B. Yilmaz, C.-B. Chae, B. Tepekule, and A. E. Pusane, "Arrival modeling and error analysis for molecular communication via diffusion with drift," in *Proc. ACM Int. Conf. on Nanoscale Comput. Commun. (NANOCOM)*, 2015, p. 26.

[14] W. Freude, R. Schmogrow, B. Nebendahl, M. Winter, A. Josten, D. Hillerkuss, S. Koenig, J. Meyer, M. Dreschmann, M. Huebner, C. Koos, J. Becker, and J. Leuthold, "Quality metrics for optical signals: Eye diagram, Q-factor, OSNR, EVM and BER," in *Proc. Int. Conf. on Transparent Opt. Netw. (ICTON)*, Jul. 2012, pp. 1–4.

[15] D. J. Schroeder, *Astronomical Optics*. Academic Press, 2000.

[16] J. E. Hall, *Guyton and Hall Textbook of Medical Physiology*, 13th ed. Elsevier, 2015.